6-12-2012

Conceptual and Mathematical Models of Batch Simultaneous Saccharification and Fermentation: Dimensionless Groups for Predicting Process Dynamics

D. Raj Raman
Iowa State University, rajraman@iastate.edu

Robert Philip Anex
Iowa State University

Conceptual and Mathematical Models of Batch Simultaneous Saccharification and Fermentation: Dimensionless Groups for Predicting Process Dynamics

Abstract
This paper describes a modeling effort demonstrating that dimensionless groupings of classical process parameters can be used to predicting process dynamics of batch simultaneous saccharification and fermentation (SSF) processes. Michaelis–Menten enzyme kinetics and Monod growth kinetics were employed, and inhibition of enzyme action and inhibition of microbial growth were neglected. The SSF process was characterized by the relative durations of three phases: A microbially-limited phase, a hydrolysis-limited phase, and a monosaccharide-depletion phase. The duration of these three phases were interrelated, and well predicted by the dimensionless magnitude of the monosaccharide peak (MSP). Thus, the MSP could be used as a single-value descriptor of an SSF process. The dimensionless ratio of the initial hydrolysis rate to the initial substrate consumption rate was shown to predict MSP, and an overall system time constant was shown to predict the total run time of a batch SSF process.

Keywords
Simultaneous-Saccharification-Fermentation, SSF, Simulation, Dimensionless-Group, Batch-Reactor

Disciplines
Agriculture | Bioresource and Agricultural Engineering

Comments
Electronic version of an article published as *Journal of Biological Systems* 20, no. 2 (June 2012): 195–211, doi:10.1142/S0218339012500064.

Conceptual and Mathematical Models of Batch Simultaneous Saccharification and Fermentation: Dimensionless Groups for Predicting Process Dynamics

D Raj Raman[1] and Robert P Anex

Abstract

This paper describes a modeling effort demonstrating that dimensionless groupings of classical process parameters can be used to predicting process dynamics of batch Simultaneous Saccharification and Fermentation (SSF) processes. Michaelis-Menten enzyme kinetics and Monod growth kinetics were employed, and inhibition of enzyme action and inhibition of microbial growth were neglected. The SSF process was characterized by the relative durations of three phases: a microbially-limited phase, a hydrolysis-limited phase, and a monosaccharide-depletion phase. The duration of these three phases were interrelated, and well predicted by the dimensionless magnitude of the monosaccharide peak (MSP). Thus, the MSP could be used as a single-value descriptor of an SSF process. The dimensionless ratio of the initial hydrolysis rate to the initial substrate consumption rate was shown to predict MSP, and an overall system time constant was shown to predict the total run time of a batch SSF process.

Keywords

Simultaneous-Saccharification-Fermentation; SSF; simulation; dimensionless-group; batch-reactor

1 Introduction

Simultaneous saccharification and fermentation (SSF) is a bioconversion process involving the hydrolysis of polysaccharides into monosaccharides in the presence of fermentative organisms that consume the simple sugars (1; 2). Compared to sequential saccharification and fermentation, SSF reduces product inhibition of hydrolytic enzymes while reduces substrate inhibition of the fermentative organisms. Along with the enzyme kinetics and microbial growth parameters, which are intrinsic to the enzymes and microbes in an SFF process, initial loading of polysaccharides, initial enzyme concentration, and microbial inoculum concentration dictate the dynamics of batch SSF processes. Together, all these process parameters will influence the changes of process variables over time – i.e., the process trajectories or dynamics – and the time needed to complete the bioconversion of polysaccharides to final products. In full-scale facilities, a combination of lab experiments and experience can establish appropriate levels of initial polysaccharide concentration, enzyme concentration, inoculum concentration, and batch retention time. However, the growing interest in biofuels has driven many labs to pursue high-throughput fermentation screening as they evaluate various feedstocks, pretreatments, enzyme cocktails, and microorganisms, and combinations thereof. Because of the large number of fermentations that may be desired, it is useful to have a process model that can allow evaluation of the interplay between the experimentally controllable variables. The development of such a

[1] Address for sending of offprints: Professor D. Raj Raman, 3222 NSRIC, Iowa State University, Ames, IA 50011-3310.

model, as well as of dimensionless groupings that could predict the system behavior, was the primary goal of this effort. These goals have not been addressed in previous modeling studies of SSF, which instead have focused on parameter estimation, on predicting maximum product concentrations, on understanding the interactions between various hydrolytic enzymes, on interrelationships between microbial and enzyme processes, on examining the sensitivity of the process to various parameters, and on the challenges of modeling cellulose hydrolysis (1; 3 – 7).

2 Materials & Methods

2.1 Approach

To achieve our goal of identifying the mathematical relationships between the relevant kinetic constants, initial concentrations of reactants, and the time and the trajectories of the process variables, we used the following approach: (a) Model the SSF process using classical equations for enzyme catalyzed reactions and microbial growth. (b) Define dimensionless groupings based upon biochemically-relevant terms. (c) Develop summary values to characterize process trajectories, thereby enabling a statistical evaluation of correlation between the proposed dimensionless groupings and the process trajectories. (d) Simulate SSF over a wide range of parameter values to develop the data set necessary to correlate process trajectories on the basis of the proposed dimensionless groupings.

2.2 Modeling SSF Using Classical Equations

To make the effort more tractable, simple models of hydrolysis and microbial growth were employed. Specifically, the Michaelis-Menten expression was used to describe hydrolysis of polysaccharides, and the Monod growth equation was used to describe the growth of microbes on monosaccharides. Further simplifying assumptions included ignoring lag-phase, ignoring the inhibitory effects of monosaccharides on enzymatic hydrolysis of polysaccharides, ignoring the inhibitory effects of monosaccharides on microbial growth, ignoring the inhibitory effects of fermentation by-products on microbial growth, and ignoring the impacts of competition from contaminating organisms. Under these assumptions, the governing differential equations for the batch SSF process were written as follow:

$$\frac{dX}{dt} = \left(\frac{\mu_{\max} S}{K_S + S} - k_d \right) X \tag{2.1}$$

$$\frac{dS}{dt} = \frac{v_{\max} C}{k_m + C} - \frac{\mu_{\max} S X}{Y_{XS}\left(K_S + S\right)} \tag{2.2}$$

$$\frac{dC}{dt} = -\frac{v_{\max} C}{k_m + C} \tag{2.3}$$

Where X represents the microbe concentration (mg L^{-1}), t represents time (h), μ_{max} represents the maximum specific growth rate of the microbes (h^{-1}), S represents the glucose concentration (mg L^{-1}), K_s represents the Monod constant (mg L^{-1}), k_d represents the first order death rate (h^{-1}), v_{max} represents the maximum reaction velocity of the hydrolysis reaction (mg L^{-1} h^{-1}), C represents the polysaccharide concentration (mg L^{-1}), k_m represents

the Michaelis (or half-velocity) constant (mg L^{-1}), and Y_{xs} represents the microbial yield per unit glucose consumed (mass/mass – dimensionless). These three coupled differential equations were implemented as a single function in MATLAB (The MathWorks, Inc., Natick, MA) and numerically integrated using a single line of code that calls a fourth-order Runge-Kutta solver. The process was simulated from t = 0 until after the peak in microbial biomass, which is also the time when polysaccharides and monosaccharides were depleted. For each run, a variety of dimensionless groupings and summary values were computed, as detailed below.

2.3 Defining Potential Dimensionless Groupings

The three governing differential equations (eq. 2.1 – 2.3) contain ten variables (q = 10) and five fundamental units (u = 5), where the mass of polysaccharide, monosaccharide, and microbes are treated as having distinct units. By the Buckingham pi theorem (e.g., 8), five independent dimensionless groupings of six core variables each are possible, resulting in 25 coefficients that must be determined. Because of the exponential nature of microbial growth, and the close relationships between some of the ten variables (e.g., S_0 and K_S), we did not pursue this enumeration of all dimensionless groupings, but rather relied upon an understanding of the processes described by the three governing differential equations to develop several possible dimensionless groups that may be used to characterize the batch SSF process. To describe these, we began by defining the following dimensionless variables:

$$C' = \frac{C}{C_0} \tag{2.4a}$$

$$S' = \frac{S}{C_0} \tag{2.4b}$$

$$X' = \frac{X}{C_0 Y_{xs}} \tag{2.4c}$$

Where C_0 is the initial, and hence maximum, polysaccharide concentration in the batch reactor, C' is dimensionless polysaccharide concentration, S' is dimensionless monosaccharide concentration, and X' is dimensionless microbe concentration, and all other variables are as previously defined. Dividing C by C_0 in equation 2.4a normalizes the polysaccharide concentration on its maximum possible value: C' begins at 1 and drops toward 0 as the batch SSF process progresses. Since the only process acting on the polysaccharide is hydrolysis, C is continually dropping as reflected by equation 2.3 which dictates $dC/dt \leq 0$. In a similar manner, dividing S by C_0 in equation 2.4b gives dimensionless monosaccharide concentration. Because there is a nearly 1:1 mass conversion ratio between mono- and polysaccharide, and because the initial monosaccharide concentration (S_0) is typically much less than C_0, C_0 represents an approximate upper bound on S. Unlike C', S' does not start at 1 and monotonically decrease, instead it would normally be expected to start at a relatively low value (approx. 1%) and vary over time depending on the relative rates of hydrolysis and consumption reflected in equation 2.2. Finally, dividing X by the maximum theoretical microbial biomass (C_0 multiplied by Y_{xs}) in equation 2.4c yields the dimensionless microbial

concentration. The C_0Y_{xs} term represents the maximum microbial biomass that could be produced in the batch reactor assuming that all initial polysaccharide is converted to monosaccharide and subsequently used for microbial growth, and assuming that the inoculum size is negligible. In reality, incomplete hydrolysis and microbial death will prevent this maximum from being attained, but as with the two previous dimensionless variables, this definition allows a critical system variable (microbial biomass) to be represented on a normalized 0 – 1 scale.

When analyzing dynamic systems it is typical to define a dimensionless time (often denoted as θ) as follows: $\theta = t/\tau$, where τ is a characteristic time (or time constant) for the system. In SSF, there are two obvious characteristic times: τ_E, a characteristic time based upon the enzymatic hydrolysis of polysaccharides, and τ_X, a characteristic time based upon the microbial growth process. More specifically, the enzymatic time constant can be thought of as the time necessary for the enzyme to completely hydrolyze the polysaccharide under ideal circumstances where v_{max} can be maintained even as substrate concentrations drop to zero. This can be computed based upon the ratio of initial polysaccharide concentration to maximum reaction velocity, as in equation 2.5a below:

$$\tau_E = \frac{C_0}{v_{\max}} \qquad (2.5a)$$

Or, it can be made slightly more complex to reflect the decrease in rate caused by non-zero half-velocity constants, as show in equation 2.5b below:

$$\tau_E = \frac{C_0 + k_m}{v_{\max}} \qquad (2.5b)$$

Notice that both of the expressions for enzymatic time constant are dependent upon a combination of intrinsic (k_m) and extrinsic (C_0) properties of the system. (The maximum reaction velocity, v_{max}, is both intrinsic and extrinsic as it reflects the enzyme turnover rate which is intrinsic, and the enzyme concentration, which is extrinsic.)

In parallel to the definitions for enzyme time constants, the microbial time constant can be thought of as the time necessary for the microbes to completely consume the monosaccharides, assuming that conversion from polysaccharides is not rate limiting, and that microbial growth is not limited by monosaccharide concentrations. In this case, the microbial growth rate can be expressed as a simplification of equation 2.1 that occurs when $S >> K_s$:

$$\frac{dX}{dt} = (\mu_{\max} - k_d)X \qquad (2.6)$$

If equation 2.6 is integrated until the maximum possible final microbe concentration (C_0Y_{XS}) is achieved, the time required to reach this maximum can be shown to be one of the two following equations, depending on whether or not k_d is included:

$$\tau_X = \frac{\ln(1 + C_0 Y_{XS} / X_0)}{\mu_{\max}} \qquad (2.7a)$$

$$\tau_X = \frac{\ln(1 + C_0 Y_{XS} / X_0)}{\mu_{max} - k_d} \quad (2.7b)$$

Both the enzyme and microbial time constants have advantages and disadvantages for use as the characteristic time for a batch SSF process. The enzyme time constant is attractive because of its simplicity and unattractive because it ignores the critical role played by microorganisms in the system. The microbial time constant captures the role of microbes, but ignores the role of enzymes and is a significantly more complex expression. Because of the difficulty in selecting between these two time constants on an *a priori* basis, we did preliminary simulations using both time constants as well as a variety of mean values of the two (arithmetic, geometric, logarithmic), examining the correlations between critical process variables and key dimensionless groups in each case. The correlations between process variables and dimensionless groups were not greatly affected by the time constant used. However, because the enzyme-based time constant was straightforward to compute and to explain, time was normalized by τ_E as defined in equation 2.5b. Because the total process duration depended on both enzymatic and microbial processes, we set the initial simulation duration on the basis of the sum of τ_E and τ_X, which we term the overall system time constant, and designate as τ.

With the time constant defined, three potential dimensionless groupings were developed based upon our understanding of the SSF process described by equations 2.1 – 2.3. They are shown below:

$$RDG_1 = \frac{v_{max} C_0 Y_{XS} (K_S + S_0)}{(k_m + C_0) S_0 X_0 \mu_{max}} \quad (2.8)$$

$$RDG_2 = \frac{v_{max}}{\mu_{max} (C_0 + S_0) Y_{XS}} \quad (2.9)$$

$$RDG_3 = \frac{\tau_X}{\tau_E} = \frac{\ln(1 + C_0 Y_{XS} / X_0) v_{max}}{(\mu_{max} - k_d)(C_0 + k_m)} \quad (2.10)$$

Equation 2.8 defines dimensionless grouping #1 (RDG_1) as the ratio of the initial hydrolysis rate to the initial substrate consumption rate. To do so, it takes the ratio of the first term to the second term in Equation 2.2, using initial values for microbial, polysaccharide, and monosaccharide concentrations, namely X_0, C_0, and S_0. Equation 2.9 defines dimensionless grouping #2 (RDG_2) as the ratio of the maximum possible hydrolysis rate to the maximum possible substrate consumption rate. The latter condition would occur if all the initial mono- and polysaccharide were converted to microbes at the yield coefficient, and if that entire microbial biomass were growing at the maximum specific growth rate. Equation 2.10 defines dimensionless grouping #3 (RDG_3) as the ratio of microbial to enzymatic time constants, which is the ratio of the time required for microbes to consume all the polysaccharide to the time required for the enzyme to hydrolyze all the polysaccharide. Initial testing showed that all three of these dimensionless groupings had some predictive value regarding the time courses of

monosaccharides during the SSF simulation. To go beyond qualitative descriptions, a method of numerically summarizing the process time courses, or trajectories, was needed.

2.4 Summary Values to Characterize Process Trajectories

Figure 1 presents a conceptual model of carbon flow during SSF. Throughout the SSF process, fermentative organisms are consuming monosaccharides, resulting in a fermentative demand (FD) that could be expressed in units of concentration per unit time. The hydrolysis of polysaccharides is the ultimate source of these monosaccharides, but accumulated monosaccharides form a second source (or sink) of monosaccharides. A mass balance on the node where these three processes meet yields the following expression:

$$MER = FD - HR \tag{2.11}$$

Where MER is the monosaccharide extraction rate (essentially the rate of depletion of the monosaccharide pool), FD is the fermentative demand, and HR is the hydrolysis rate, as shown in Figure 1. The sign of the monosaccharide extraction rate, and its magnitude compared with the hydrolysis rate, can then be used to characterize the batch SSF process, as detailed below.

Figure 2 presents concentrations of polysaccharides, monosaccharides, and microbes as functions of dimensionless time for a single simulation, and illustrates key features of the trajectories of each of these variables during a batch SSF process. The dimensionless polysaccharide concentration starts at 1.0 and decreases to nearly zero at a dimensionless time of 1.0. The decrease in polysaccharide concentration is almost linear because the rate of hydrolysis is near v_{max} until the polysaccharide concentration is low with respect to k_m. The microbial concentration begins at the inoculum concentration and increases exponentially as monosaccharides accumulate. However, because of the exponential nature of microbial growth, the hydrolysis rate – which is virtually constant at v_{max} – cannot keep up with the fermentative demand indefinitely, and the monosaccharide concentration eventually peaks and begins decreasing as microbial consumption outstrips production. This occurs at $\theta = 0.81$ in the particular system represented in Figure 2. This peak in monosaccharides marks the end of what we refer to as Phase 1, the *microbially-limited* phase of the SSF. Using the nomenclature from Figure 1, we defined Phase 1 as a time when HR > FD, making MER < 0 and resulting in monosaccharide accumulation.

From $\theta = 0.8$ till $\theta = 1.18$, the process illustrated in Figure 2 is in what we refer to as Phase 2, the *hydrolysis-limited* phase. During this phase, the hydrolysis rate is no longer greater than the fermentative demand. However, the hydrolysis rate still exceeds the monosaccharide extraction rate during Phase 2, so hydrolysis is still considered to be limiting. Using the nomenclature from Figure 1, we defined Phase 2 as a time when HR > MER > 0, resulting in some depletion of the monosaccharide pool, but with hydrolysis continuing to account for the majority of the fermentative demand, since HR > MER.

Finally, from $\theta = 1.18$ till $\theta = 1.89$, the hydrolysis rate drops below the rate of extraction of the monosaccharide pool (the organism are now living primarily on “savings” rather than “income”), and the process illustrated in Figure 2 is in Phase 3, termed the

monosaccharide-depletion phase. Using the nomenclature from Figure 1, we defined Phase 3 as a time when HR < MER, resulting in depletion of the monosaccharide pool with hydrolysis playing a minor role in meeting the fermentative demand.

Not all SSF processes will progress through all three phases. For example, a system with a rapidly growing microbe at high initial titers coupled with low overall hydrolysis rates will not exhibit a significant peak in monosaccharides. Such a system primarily operates in Phase 2 for the entirety of the process. At the other extreme, if hydrolysis rates are much larger than initial microbial demand, the peak in monosaccharides may occur near, or even after, the polysaccharide is depleted. Such a system only operates in Phases 1 and 3, and never in the hydrolysis-limited Phase 2.

The end of Phase 1 was defined as the dimensionless time of the peak value in the dimensionless monosaccharide concentration, and the end of Phase 3 was defined as the dimensionless time of the peak value in the dimensionless microbe concentration. (The total treatment time was simply the actual time of the peak value in the dimensionless microbe concentration.) The end of Phase 2 was identified as the time at which monosaccharide depletion rates exceeded hydrolysis rates: if this time coincided with the end of Phase 1, then there was effectively no Phase 2. At the other extreme, if this time coincided with the end of Phase 3, then there was effectively no Phase 3. In all cases, we took the length of each phase and normalized it by the overall process duration (i.e., the end of Phase 3). We refer to these as the "relative durations" of each phase.

A variety of potential characteristic values were considered as summary descriptors of process trajectory. We focused our attention on the relative duration of each of the three phases, upon the dimensionless magnitude of the sugar peak, and upon the total run time. Together, these comprise an easy to comprehend summary of the trajectory of a batch SSF process, in the absence of any substrate or product inhibition effects.

2.5 Ranges of Process Variables

A process simulation was run for a wide range of SSF fundamental kinetic parameters as shown in Table 1. The simulation was run until a peak in microbial biomass was observed. Enzyme parameter values were based on starch hydrolysis by crude amylase preparations and microbial growth parameter values were based on those reported for yeast. Each variable was uniformly distributed within the range shown in Table 1, and the simulation was repeated 10^4 times. The following values were abstracted for each simulation: dimensionless maximum value of the monosaccharide peak, total run time, relative durations of all three phases, enzyme time constant, microbial time constant, total system time constant ($\tau_E + \tau_X$), and all three proposed dimensionless groups.

3 Results & Discussion

A small number (approximately 0.5%) of simulation runs were not amenable to categorization because the microbial populations monotonically decreased due to low hydrolysis rates or large inocula sizes relative to polysaccharide loadings. Because these

conditions would not normally be used by researchers, these anomalous simulation runs were automatically eliminated from the analysis. In the 10^4 simulation runs, a wide variety of trajectories were seen, from Phase-2 dominated runs with small monosaccharide peaks, to those with moderate monosaccharide peaks as previously illustrated in Figure 2, to those with extreme monosaccharide peaks, and no discernable Phase 2. The simulations clearly capture important dynamics in actual SSF processes, as evidenced by comparison to SSF process trajectories in the literature (e.g., 3; 10; 18).

The dimensionless monosaccharide peak (MSP), found by normalizing the actual monosaccharide peak by the initial polymer concentration, was a strong predictor of the relative duration of Phase 1 (P1D), as illustrated in Figure 3. This behavior was unsurprising considering the biochemical basis of MSP and P1D, specifically: Low values of the monosaccharide peak indicate that demand from microbial growth rapidly surpasses production via hydrolysis, leading to a short relative duration of Phase 1, as indicated on the far left of Figure 3. At intermediate values of MSP (e.g., trajectory illustrated previously in Figure 2), Phase 1 has a relatively long duration – ranging from 30 – 60% of the total batch time. At the highest values of MSP, although the total duration of Phase 1 is nearly 1.0 dimensionless time units, its relative duration is low because the overall batch time is dominated by a protracted Phase 3. This explains the tendency for P1D to decrease in the upper half of MSP's range.

The parabolic shape of Phase 1 Duration as a function of monosaccharide peak magnitude hints at the shapes of the other two phases, because the sum of the three phase durations must be unity. Figures 4A and 4B illustrate this interrelationship clearly, with Phase 2 dominating at low levels of monosaccharide peak (Figure 4A), but decreasing steadily with increasing MSP, and with Phase 3 showing exactly the opposite effect. Both Phase 2 and 3 durations slow a slight bifurcation in the MSP range of 0.1 to 0.3, reflecting the occasional possibility for a moderate monosaccharide peak to be followed by a brief Phase 2 and long Phase 3, instead of the more common long Phase 2.

Although the bifurcations in Figure 4 A and B confounds interpretation slightly, the monosaccharide peak can be used to predict the relative lengths of the three phases of a batch SSF, and as such is a straightforward descriptor of such processes. Table 2 provides a guide to interpreting the SSF trajectories based on the monosaccharide peak.

We have argued here that the monosaccharide peak is a good single-value descriptor of batch SSF processes, insofar as it provides insight into the trajectories of key process quantities. In addition to knowledge of the monosaccharide peak, knowledge of the overall run time is critical. In our simulations, we identified overall run time as the time at which microbial concentrations peak, which is coincident with the exhaustion of polysaccharide and monosaccharide substrates. The total run time and monosaccharide peak can be used as design criteria for experimentalists running high numbers of batch SSF processes, for example – total run time of 36 h and a maximum monosaccharide peak of 5% to ensure that the process proceeds primarily in a hydrolysis-limited regime.

One way of meeting such criteria is to simulate the process and to iterate on easily manipulated variables such as enzyme concentration and inoculum size until the desired trajectory is achieved. However, the process would be streamlined if easily computed parameters could be used to predict total run time and monosaccharide peak size. Regression analysis of the data indicated that the strongest predictor of the total run time was the overall time constant ($\tau = \tau_E + \tau_X$). The overall system time constant predicts the total treatment time with $r^2 = 0.82$, with the caveat that there is a large variation in total treatment time about the 1:1 line. This result confirms that both enzyme loading and inoculum size – which together drive the τ_E and τ_X values – are crucial to the overall time required for an SSF process to run to completion.

Linear regression of each of the three proposed dimensionless groups on the monosaccharide peak yielded mixed misleading results, in part because of the non-linearity evident in these relations (data not shown). However, closer examination of the relationship between the dimensionless groups and the monosaccharide peak in the low (< 0.1) range of monosaccharide peaks showed that RDG_1 was a strong predictor of monosaccharide peak in this range (Figure 5), with a correlation coefficient above 0.8. In contrast, RDG_2 and RDG_3 had correlations of 0.07 and 0.3, respectively, and were therefore poor predictors of the monosaccharide peak.

Examination of Figure 5 suggested that using a range of $1 < RDG_1 < 5$ would reliably keep MSP from exceeding 0.1. When this limitation was placed on the process, the variation in treatment time vs. overall time constant dropped greatly, as shown in Figure 6. Furthermore, in this range the overall system time constant was a reliable upper bound on treatment time, making it an even more useful predictor of the process trajectory.

The first proposed dimensionless group, RDG_1, appears to be an excellent predictor of simulated batch SSF process trajectories. Computation of RDG_1 should be relatively straightforward for most well-characterized microbial and enzyme systems. For batch SSF processes where a low peak in monosaccharides is desirable, we recommend selecting initial concentrations of polysaccharide, monosaccharide, and microbes such that RDG_1 is in the range of 1 to 5, depending on the maximum acceptable monosaccharide concentration.

Rearranging equation 2.8 to clarify the relationships between experimentally selectable variables and RDG1 yields:

$$RDG_1 = \left\{\frac{C_0}{k_m + C_0}\right\}\left\{\frac{K_S + S_0}{S_0}\right\}\left\{\frac{v_{max}}{X_0}\right\}\left\{\frac{Y_{XS}}{\mu_{max}}\right\} \qquad (3.1)$$

The first bracketed term will typically have a value close to unity (1.0) and be relatively insensitive to changes in C_0, because C_0 would normally be significantly greater than k_m. In contrast, the second bracketed term is normally sensitive to S_0, because S_0 would be on the same order of magnitude as K_s. Both of the terms in the third bracket, v_{max} and X_0,

could be manipulated to achieve a desired value of RDG_1, whereas the final bracketed term is not within experimental control. Other investigators have noted the importance of inoculum size (X_0) on the trajectory of SSF processes (19). Once an experimentalist had selected operating conditions to achieve a desired value of RDG_1 within the 1 – 5 range, a robust estimate of the total run time can be made by computing the overall system time constant, and experimental parameters can be adjusted to meet a desired total run time per equation 3.2 below:

$$\tau = \frac{(C_0 + k_m)}{v_{max}} + \frac{\ln(1 + C_0 Y_{XS} / X_0)}{(\mu_{max} - k_d)} \qquad (3.2)$$

Notice that adjustments to C_0 are an effective method of altering the overall time constant while only slightly influencing RDG_1. In contrast, RDG_1 is highly sensitive to changes in v_{max} or X_0, complicating adjustment of the system time constant by changing either of these variables.

Under the assumptions of the model, RDG_1 and the overall time constant (τ) appear to have value in the prediction of SSF process trajectories, which are well summarized by the dimensionless magnitude of the monosaccharide peak. However, a variety of simplifying assumptions were made to arrive at this initial goal. For example, this model assumes that a single hydrolysis product is produced, and that only this product is a viable feedstock for the microbe – an assumption that is not valid for the standard SSF processes used in dry-grind ethanol plants, where enzymes mediate a multi-step starch hydrolysis process, and where multiple hydrolysis products are viable feedstocks for the yeast. Future work should systematically develop more complex systems of equations that remove these constraints. Specifically, inclusion of a lag-phase, inclusion of product inhibition of the hydrolysis enzymes, and inhibition of microbial growth by monosaccharides and fermentation by-products should all be incorporated. For modeling cellulosic ethanol SSF processes, the Michaelis-Menten formalism should be replaced with more appropriate models (e.g., 20). As any of these complexities are added, new dimensionless groupings must be explored. We believe that this work provides a useful framework for such explorations.

4 Conclusions

Batch SSF process dynamics can be summarized by the monosaccharide peak magnitude, the microbially-limited, hydrolysis-limited, and monosaccharide-depletion phase lengths, and the total run time, with the first four of these being closely interrelated. The process dynamics can be summarized by the magnitude of the monosaccharide peak, and these dynamics can be predicted by a dimensionless grouping of process variables. An overall system time constant can be computed by summing the enzymatic and microbial time constants, and can predict the total run time of a batch SSF process.

5 Acknowledgements

The authors wish to thank Asli Isci, Patrick Murphy, and Lisa Haney for their lab-scale work that motivated the development of this paper. This material is based in part upon work supported by the National Science Foundation under Award No. EEC-0813570, and

by the United States Department of Agriculture Award No. 2006-38411-17034. Any opinions, findings, and conclusions or recommendations expressed in this material are those of the author(s) and do not necessarily reflect the views of the National Science Foundation or of the United States Department of Agriculture.

6 References

1. Philippidis GP, Spindler DD, Wyman CE, Mathematical modeling of cellulose conversion to ethanol by the simultaneous saccharification and fermentation process, *Applied Biochemistry and Biotechnology* **34/35**, 543 – 556, 1992.
2. Takagi M, Suzuki S, Gauss WF, Manufacture of Alcohol from Cellulosic Materials Using Plural Ferments, United States Patent No. 3,990,944, 1976.
3. Anuradha R, Suresh AK, Venkatesh KV, Simultaneous saccharification and fermentation of starch to lactic acid, *Process Biochemistry* **35**(3-4), 367 – 375, 1999.
4. Philippidis GP, Smith TK, Wyman CE, Study of the enzymatic hydrolysis of cellulose for production of fuel ethanol by the simultaneous saccharification and fermentation process, *Biotechnology and Bioengineering* **41**, 846 – 853, 1992.
5. Ramachandran KB, Hashim MA, Simulation studies on simultaneous saccharification and fermentation of cellulose to ethanol, *The Chemical Engineering Journal* **45**(2): B27 – B34, 1990.
6. Rivas B, Moldes AB, Dominguez JM, Parajo JC, Lactic acid production from corn cobs by simultaneous saccharification and fermentation: a mathematical interpretation. *Enzyme and Microbial Technology* **34**(7), 627 – 634, 2004.
7. South CR, Hogsett DAL, Lynd LR, Modeling simultaneous saccharification and fermentation of lignocellulose to ethanol in batch and continuous reactors. *Enzyme and Microbial Technology* **17**(9), 797 – 803, 1995.
8. Geankoplis CJ, Transport Processes and Unit Operations. 3rd ed. R. P. Rottino, ed. Prentice–Hall, Inc., Englewood Cliffs, NJ, 1993.
9. Polakovic M, Bryjak J, Modeling of potato starch saccharification by an *Aspergillus niger* glucoamylase, *Biochemical Engineering Journal* **18**(1), 57 – 63, 2004.
10. Rajoka MI, Yasmin A, Latif F, Kinetics of enhanced ethanol productivity using raw starch hydrolyzing glucoamylase from *Aspergillus niger* mutant produced in solid state fermentation, *Letters in Applied Microbiology* **39**, 13 – 18, 2004.
11. Altintas MM, Ulgen KO, Kirdar B, Onsan ZI, Oliver SG, Improvement of ethanol production from starch by recombinant yeast through manipulation of environmental factors. *Enzyme and Microbial Technology* **31**(5), 640 – 647, 2002.
12. Dan NP, Visvanathan C, Basu B, Comparative evaluation of yeast and bacterial treatment of high salinity wastewater based on biokinetic coefficients, *Bioresource Technology* **87**(1), 51 – 56, 2002.
13. Gupthar AS, Bhattacharya S, Basu TK, Evaluation of the maximum specific growth rate of a yeast indicating non-linear growth trends in batch culture, *World Journal of Microbiology & Biotechnology* **16**(7), 613 – 616, 2001.
14. Van Hoek P, Van Dijken JP, Pronk JT, Effect of specific growth rate on fermentative capacity of baker's yeast, *Applied and Environmental Microbiology* **64**(11), 4226 – 4233, 1998.

15. Tchobanoglous G, Burton F, Wastewater Engineering: Treatment, Disposal, and Reuse, pp 426. Metcalf & Eddy Inc. 3rd ed. McGraw-Hill Inc., New York, 1991.
16. Najafpour G, Younesi H, Ismail KSK, Ethanol fermentation in an immobilized cell reactor using *Saccharomyces cerevisiae*, *Bioresource Technology* **92**(3), 251 – 260, 2004.
17. Silva CLC, Rosa CA, Oliveira ES, Studies on the kinetic parameters for alcoholic fermentation by flocculent *Saccharomyces cerevisiae* strains and non-hydrogen sulfide-producing strains, *World Journal of Microbiology & Biotechnology* **22**(8), 857 – 863, 2006.
18. Hofvendahl K, Akerberg C, Zacchi G, Hahn-Hagerdal B, Simultaneous enzymatic wheat starch saccharification and fermentation to lactic acid by *Lactococcus lactis*. *Applied Microbiology and Biotechnology* **52**(2), 163 – 169, 1999.
19. Vega JL, Navarro AR, Clausen EC, Gaddy JL, Effects of inoculum size on ethanol inhibition modeling and other fermentation parameters, *Biotechnology and Bioengineering* **29**(5) 633 – 638, 2004.
20. Lynd LR, Weimer PJ, van Zyl WH, Pretorius IS, Microbial Cellulose Utilization: Fundamentals and Biotechnology. *Microbiology and Molecular Biology Reviews* **66**(3), 506 – 577, 2002.

6 Figures

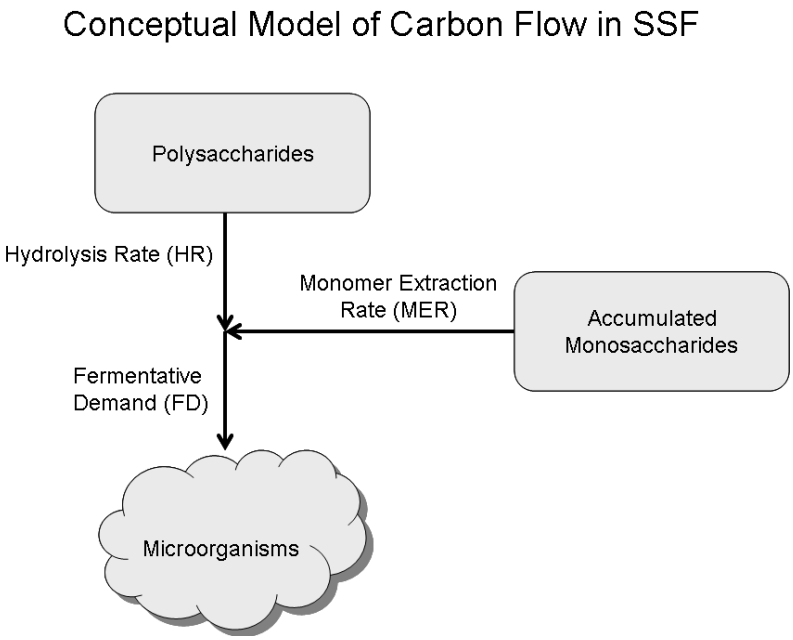

Figure 1. Conceptual model for understanding carbon flow in SSF processes. Arrows represent direction of mass flow. Hydrolysis Rate and Fermentative Demand are always positive (or zero), whereas Monomer Extraction Rate can be either positive or negative, depending on the difference between hydrolysis rate and fermentative demand. Details in text.

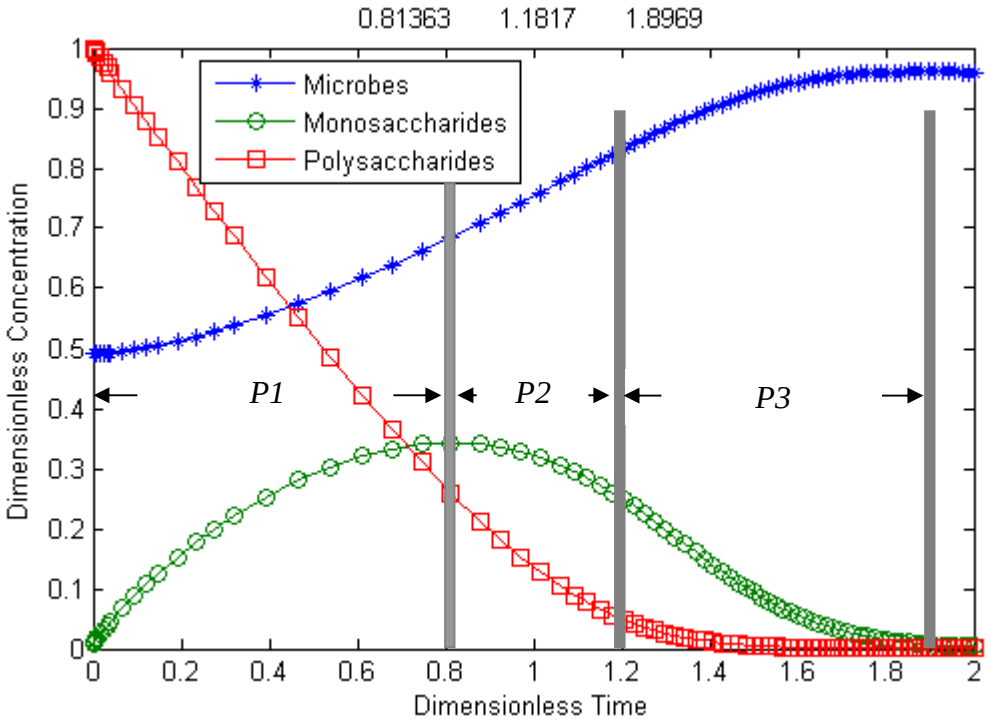

Figure 2. Sample output from SSF simulation, illustrating trajectory of microbes, monosaccharides, and polysaccharides over dimensionless time. Vertical axis represents dimensionless microbe, monosaccharide, or polysaccharide concentration. Variable symbol spacing reflects adaptive step-size routine of numerical integration method. P1 is Phase 1, the microbially-limited phase; P2 is Phase 2, the hydrolysis-limited phase; and P3 is Phase 3, the monosaccharide depletion phase. Details in text.

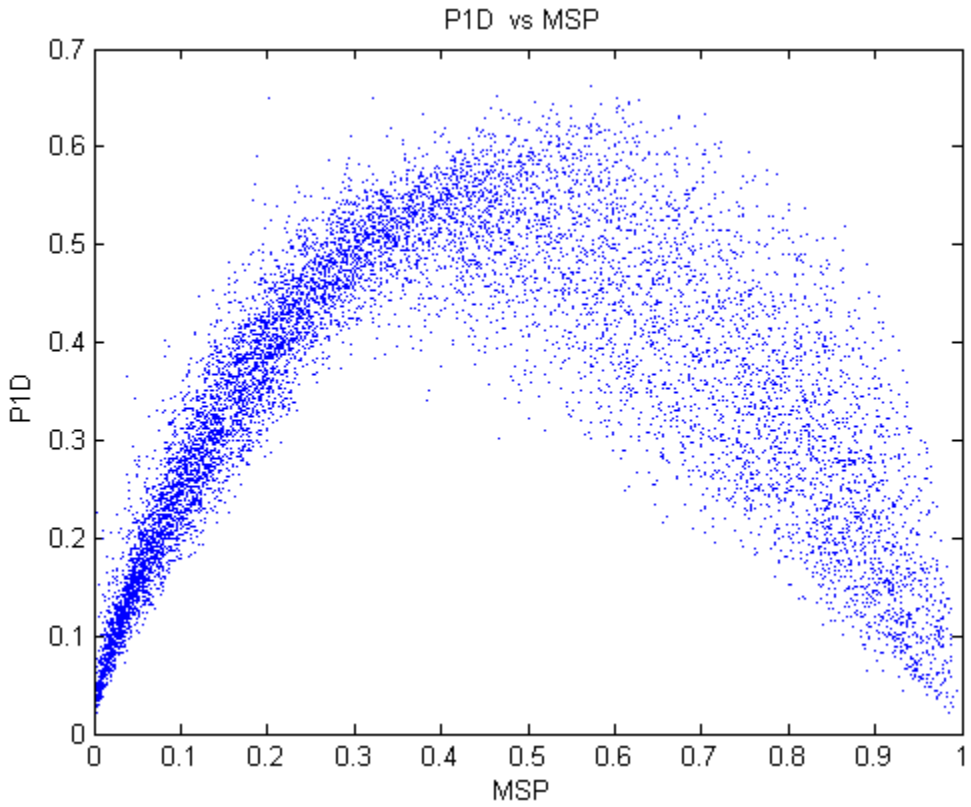

Figure 3. Relationship between Phase 1 duration (P1D) and magnitude of monosaccharide peak (MSP) for 10^4 simulations using the kinetic parameters listed in Table 1.

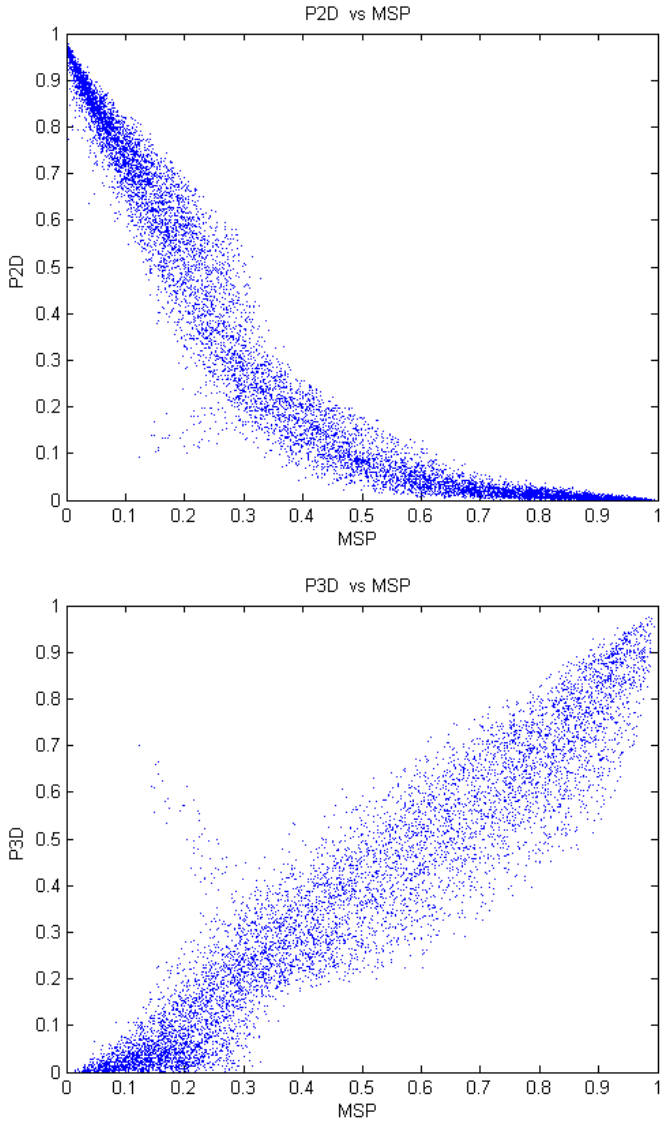

Figures 4 A & B. Relationship between Phase 2 and 3 duration (P2D and P3D) and magnitude of monosaccharide peak (MSP) for 10^4 simulations using the kinetic parameters listed in Table 1. See text for discussion.

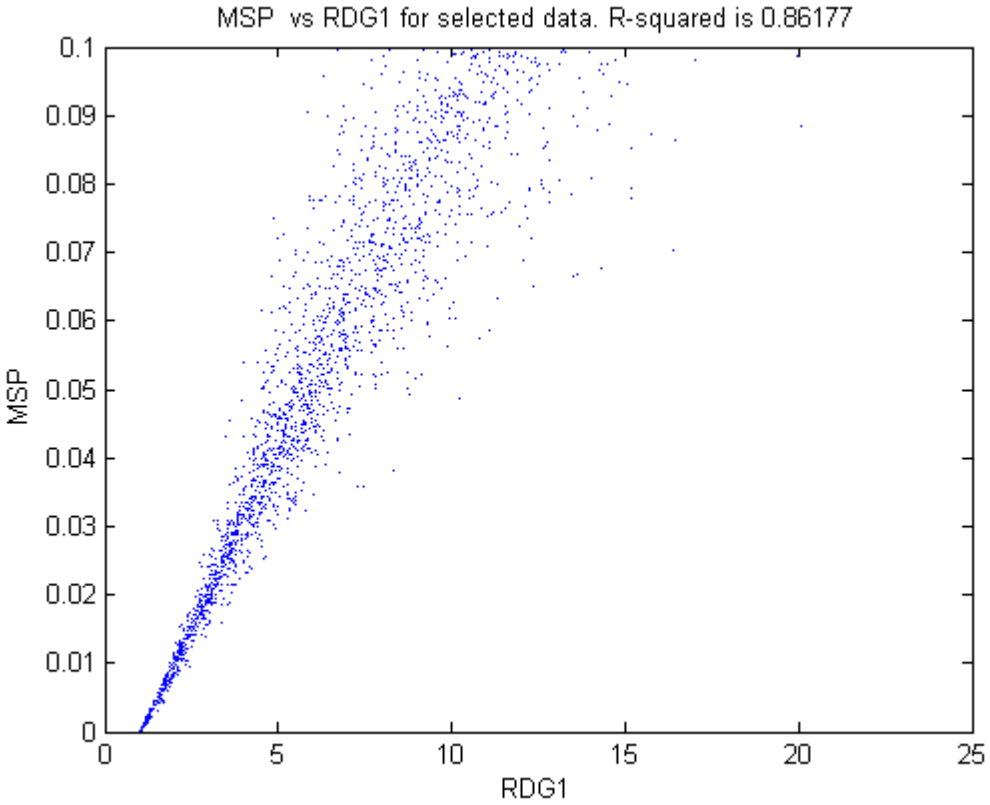

Figure 5. Relationship between monosaccharide peak and RDG_1 for subset of simulations with MSP < 0.1. (Total number of points was 2005 out of the 10,000 runs.) In this range, RDG_1 is a strong predictor of MSP, as reflected by the high value correlation coefficient (r^2 = 0.86).

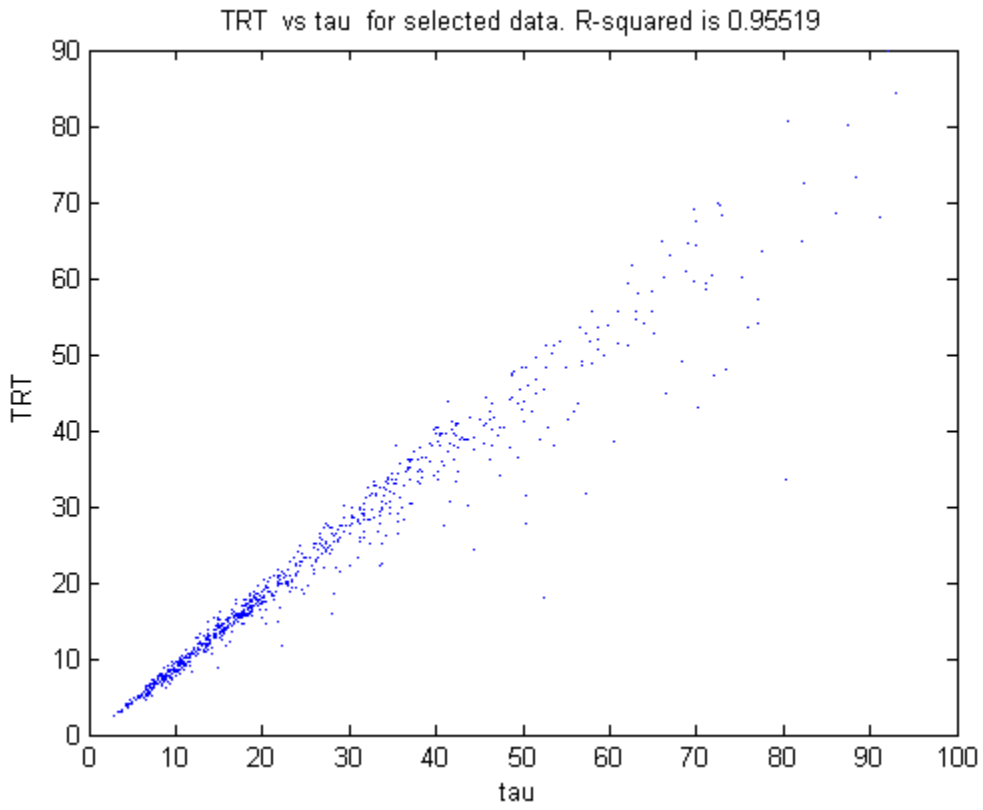

Figure 6. Relationship between total run time (TRT, units of hours) and overall time constant (tau = sum of enzyme and microbial time constants, units of hours) for subset of simulations with $1 < RDG_1 < 5$. (Total number of points was 819 out of the 10,000 runs.) Within this subgroup, the overall time constant is an excellent predictor of the total run time, as reflected by the 0.95 correlation coefficient.

7 Tables

Table 1. Ranges of values of kinetic parameters for SSF

Parameter	Range	Comments	Reference
C_0	1000 – 20,000 mg/L	Range from dilute (1%) to rich (20%) initial polysaccharide concentrations.	
v_{max}	200 – 4,000 mg/L/h	Under the assumption of Michaelis Menten kinetics, this is completely dependent upon the amount of total enzyme used, so the low value was set as C_{0min}/5 h, and high value as C_{0max}/5 h	
k_m	50 – 450 mg/L	Approximately 35% - 300% of value reported in reference. Also includes value reported in second reference.	9; 10
X_0	50 – 500 mg/L	Approximate range shown in reference.	11
S_0	1% of C_0 value (10 – 200 mg/L)	Need a small initial amount to avoid crashing microbial population during early part of simulation	
μ_{max}	0.1 - 1.2 h^{-1}	From 25% to 300% max value reported for *S. cerevisiae* in reference first. This range bounds values reported in other references.	12; 13; 14
k_d	0.01 – 0.1 μ_{max}	Bounds value reported for carbohydrate wastes	15
K_s	500 – 5000 mg/L	Range about values reported in literature	16
Y_{xs}	0.12 – 0.5 g g^{-1}	Covers range reported for *S. cerevisiae* in reference. Tends to be inversely proportional to v_{max} but treat as completely independent for simulation.	14; 17

Table 2. Interpretation of monosaccharide peak values

Monosaccharide Peak (range)	**Interpretation**
0 – 0.1	Hydrolysis is relatively slow compared to microbial growth. Relative duration of Phase 1 is short: typically less than a third of the total run time. Relative duration of Phase 2 dominates, so that the process is operating in a hydrolysis-limited regime. Relative duration of Phase 3 is brief.
0.1 – 0.5	Hydrolysis and microbial growth are occurring at similar rates – early in the process hydrolysis is sufficiently faster that significant monosaccharide accumulation occurs. Relative duration of Phase 1 is significant: typically from one third to two thirds of total, and increasing with increasing values of monosaccharide peak. Relative duration of Phase 2 is significant but dropping throughout this range. Relative duration of Phase 3 increases with increasing monosaccharide peak in this range.
>0.5	Hydrolysis has occurred extremely rapidly leading to a large peak in monosaccharides. Relative duration of Phase 1 is well over 50% when the monosaccharide peak is 50%, but decreases as monosaccharide peak increases toward 100%, because Phase 3 relative duration dominates. As is fitting for a case where hydrolysis is extremely rapid, the hydrolysis-limited Phase 2 continues to decrease with increasing monosaccharide peak throughout this range.